Computer Applications in Electrical Engineering
Vol. 14 *2016*
DOI 10.21008/j.1508-4248.2016.0003

Calculations of the magnetic field of the three-phase 4-conductor line with rectangular busbars

Dariusz Kusiak, Zygmunt Piątek, Tomasz Szczegielniak, Paweł Jabłoński
Czestochowa University of Technology
42–200 Częstochowa, ul. Dąbrowskiego 69, e–mail: dariuszkusiak@wp.pl, zygmunt.piatek@interia.pl, szczegielniakt@interia.pl, yaboo@el.pcz.czest.pl

The paper presents the results of the calculations of the magnetic field for the both shielded and non-shielded 3-phase MR 250 busbar manufactured by Elektromontaż 2 in Katowice, Poland. The busbar magnetic field has been determined by the following methods: analytical method for non–shielded busbar without taking into account the skin and proximity effects, analytical–numerical method based on integral equations, two-dimensional method of finite elements with the use of the commercial FEMM software, measurement method on a test stand. The measurements were performed with the use of a special non-directional magnetic field meter. A satisfactory compliance of the calculations has been obtained.

KEYWORDS: magnetic field, rectangular busbar, high-current busduct

1. Introduction

Electrical connections leading considerable currents between large devices and apparatus in substations and industrial plants are usually made from aluminum or copper bare conductors (called bus bars) mounted on stand-off insulators. The bus bar systems are often enclosed in shields. Nominal currents of presently installed bus bars, both shielded and unshielded, reach up to 10 kA. Consequently, magnetic field intensity generated by such bus bars is relatively large, even at nominal currents. The magnetic fields affect the bus bar system elements and its neighborhood – other electrical devices and apparatus, steel constructions, electronic control and data transmission systems, natural environment and personnel. Exceeding the permissible values of magnetic field intensity can lead to incorrect functioning of electrical equipment, overheating the steel constructions, and even degradation of natural environment including threatening the human health. All the mentioned problems can be discussed in the terms of electromagnetic compatibility, which requires determination of magnetic field intensity around devices generating it. Besides, the knowledge of magnetic field in the systems is often required due to the environment and personnel safety [1].

The present trends in use of rectangular bus bar systems seem to confirm their increasing usefulness in medium and high voltage electrical substations. Particularly large increase of their importance can be noticed for low voltage bus bar systems, which are the main supply systems in industrial plants. The today production is often aimed to short series. As a consequence, this requires frequent rearrangements in production line, which enforces changes in supply system. This can be a big and expensive problem in case of cable supply, but can be practically eliminated if the machinery power supply is lead from bus bar system with tap-off boxes [2, 3]. In each case, it is necessary to check if the magnetic field intensity does not exceed permissible values indicated by standards and law. This requires measurements around bus bar systems. Measurements of magnetic field in such systems can be troublesome due to inaccessible places under the shield. This paper shows a use of measurement system with a non–directional probe of special construction in magnetic field measurements around a three-phase bus bar system. Apart from measurements, also computations were performed, and the results are discussed below.

The subject of the investigation was the busbar of MR 250 type and its two versions: the unshielded busbar and the shielded one. The dimensions for those solutions are: $a = 7$ mm, $b = 16$ mm and $d = d_1 = 26$ mm (Fig. 1). The phase busbars and the neutral one are made of copper with the conductivity $\sigma = 56$ MS·m^{-1}. The enclosure of the busbar is made of galvanized sheet with the conductivity $\sigma_5 = 16$ MS·m^{-1} , and the thickens of its walls is t = 1 mm. The position of the enclosure walls in respect to the busbars is determined by $a_1 = b_1 = b_2 = 20$ mm.

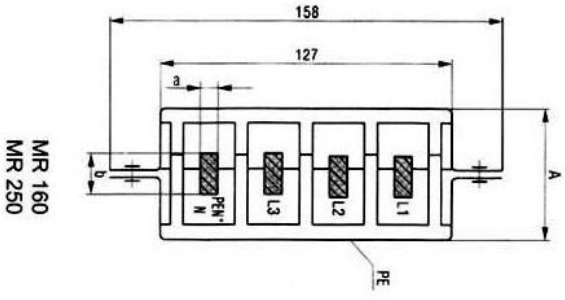

Typ przewodu szynowego	Wymiar A (mm)	Wymiar szyn a*b (mm)
MR 160	58	7*7
MR 250	58	7*16
MR 400	78	7*36
MR 630	102	7*60
MR 720	122	7*80
MR 800	122	7*80
MR 830	142	7*100
MR 1000	142	7*100

* zależne od układu sieciowego

Fig. 1. The busbar of MR type [4]

In the paper the results of the calculations and the measurements of the electromagnetic field generated by the 3–phase both unshielded and shielded 4–conductor busbar of MR 250 type, produced by Elektromontaż no. 2 in Katowice are presented.

2. Electromagnetic field of the 3-phase line generated by 4-conductor long rectangular busbars

Let us consider a 4-conductor high-current line built of rectangular busbars (Fig. 2) and with current asymmetry: $\underline{I}_1 = \underline{I}\,\mathrm{e}^{\mathrm{j}0^\circ}$, $\underline{I}_2 = 0.5\,\underline{I}\,\mathrm{e}^{-\mathrm{j}120^\circ}$, $\underline{I}_3 = \underline{I}\,\mathrm{e}^{\mathrm{j}120^\circ}$ and the current in the neutral busbar $\underline{I}_N = \underline{I}_1 + \underline{I}_2 + \underline{I}_3 = 0.5\underline{I}\,\mathrm{e}^{\mathrm{j}60^\circ}$.

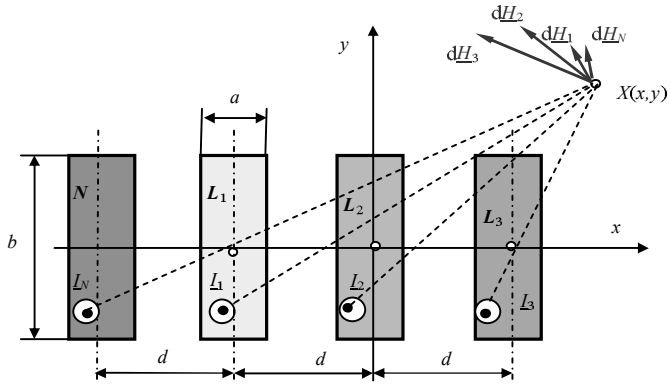

Fig. 2. The 3–phase 4–conductor line built of rectangular busbars with $\underline{I}_1$, $\underline{I}_2$, $\underline{I}_3$ and $\underline{I}_N$ currents

In this case the total elementary field in the $X(x,y)$ point generated by the currents in the elementary areas of the phase conductors and the neutral one is [5-8]

$$\mathrm{d}\underline{\boldsymbol{H}} = \mathrm{d}\underline{\boldsymbol{H}}_1 + \mathrm{d}\underline{\boldsymbol{H}}_2 + \mathrm{d}\underline{\boldsymbol{H}}_3 + \mathrm{d}\underline{\boldsymbol{H}}_N \tag{1}$$

whereas the total electromagnetic field in this point

$$\begin{aligned}\underline{\boldsymbol{H}} &= \left(\underline{H}_{x1} + \underline{H}_{x2} + \underline{H}_{x3} + \underline{H}_{xN}\right)\mathbf{1}_x + \left(\underline{H}_{y1} + \underline{H}_{y2} + \underline{H}_{y3} + \underline{H}_{yN}\right)\mathbf{1}_y = \\ &= \underline{H}_x\,\mathbf{1}_x + \underline{H}_y\,\mathbf{1}_y\end{aligned} \tag{2}$$

where the $\underline{H}_{x2}$ and $\underline{H}_{y2}$ components can be expressed by the formulas

$$\begin{aligned}\underline{H}_x(x,y) = {} & \frac{\underline{I}}{8\pi a b}\times \\ & \times\left\{\begin{aligned}&2(b-2y)\left[\operatorname{arctg}\frac{a-2x}{b-2y}+\operatorname{arctg}\frac{a+2x}{b-2y}\right]-2(b+2y)\left[\operatorname{arctg}\frac{a-2x}{b+2y}+\operatorname{arctg}\frac{a+2x}{b+2y}\right]+\\ &+(a+2x)\ln\frac{(a+2x)^2+(b-2y)^2}{(a+2x)^2+(b+2y)^2}+(a-2x)\ln\frac{(a-2x)^2+(b-2y)^2}{(a-2x)^2+(b+2y)^2}\end{aligned}\right\}\end{aligned} \tag{3}$$

and

$$\underline{H}_y(x,y)=\frac{\underline{I}}{8\pi ab}\times$$
$$\times\left\{\begin{array}{l}-2(a-2x)\left[\operatorname{arctg}\frac{b-2y}{a-2x}+\operatorname{arctg}\frac{b+2y}{a-2x}\right]+2(a+2x)\left[\operatorname{arctg}\frac{b-2y}{a+2x}+\operatorname{arctg}\frac{b+2y}{a+2x}\right]-\\ -(b+2y)\ln\frac{(a-2x)^2+(b+2y)^2}{(a+2x)^2+(b+2y)^2}-(b-2y)\ln\frac{(a-2x)^2+(b-2y)^2}{(a+2x)^2+(b-2y)^2}\end{array}\right\} \quad (4)$$

when assuming the current in them as $\underline{I}=\underline{I}_2$. The $\underline{H}_{x1}$ and $\underline{H}_{y1}$ components can be expressed by the formulas (3) and (4), after replacing the x variable by $x+d$ and assuming the $\underline{I}=\underline{I}_1$ current, the $\underline{H}_{x3}$ and $\underline{H}_{y3}$ components can be expressed by the formulas (3) and (4), respectively, after replacing the x variable by $x-d$ and assuming that $\underline{I}=\underline{I}_3$.

The $\underline{H}_{xN}$ and $\underline{H}_{yN}$ components can be expressed by the formulas (3) and (4), respectively, after replacing the x variable in them by $x+2d$ and assuming the $\underline{I}_N=\underline{I}_1+\underline{I}_2+\underline{I}_3$ current. The distributions of the magnetic field in such current line for the current asymmetry case are presented in Fig. 3 and Fig. 4.

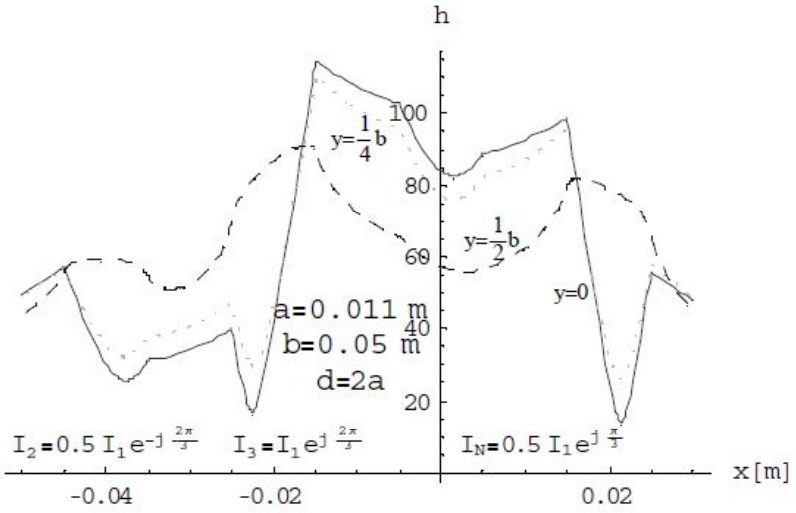

Fig. 3. The distribution of the magnetic field module of the 4–conductor 3–phase line with rectangular busbars on the plane of the cross–section of the line for the case of asymmetric currents; $a = 0.01\,\mathrm{m}$, $b = 0.05\,\mathrm{m}$, $d = 2a$

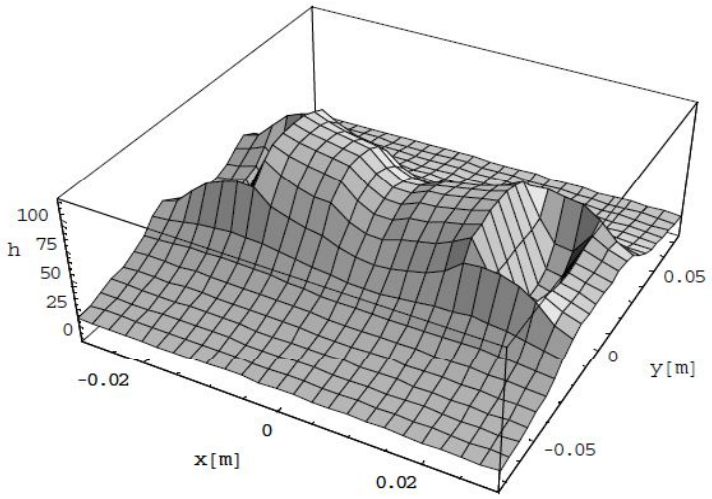

Fig. 4. The distribution of the magnetic field module of 4-conductor 3-phase line with rectangular busbars for the case of asymmetric currents; $a = 0.01\,\mathrm{m}$, $b = 0.05\,\mathrm{m}$, $d = 2a$

3. Measurement system

Excluding special cases, e.g. when the conductors are parallel and phases of their currents differ by π, the magnetic field around a system of time harmonic currents is an elliptic field. This certainly occurs in three phase systems, and is emphasized by skin and proximity effects [9, 10]. Hence, it must be taken into account during measurements. The measurement of elliptical magnetic field with use of directional probes is onerous, because the operator has to find maximum at each probing point. This requires time, attention and precision, and can generate large measurement errors due to weariness and inattention. Therefore, special non–directional probes are often constructed. One of such constructions is a specific meter for non–directional measurement of magnetic field intensity or magnetic flux density constructed as research project N N511 312540 financed by the Polish National Science Centre [11, 12] – Fig. 5.

The main part of the probe is a three–axial coil head (Fig. 6) coupled with a converter co–operating with a PC via an Ethernet interface. By using such a head of three mutually perpendicular detectors of magnetic field, the orientation of the head does not affect the detected value of magnetic field, which allows us to determine correctly the magnitudes of magnetic field intensity or magnetic flux density at any orientation of the probe head (provided that its center maintains the same required position). This makes the measurement much more easier when compared to directional probes. In addition, such a construction offers freedom in manipulating the probe during measurements. However, these advantages must be confronted with a drawback,

which is the size of the head (the diameter is about 1 cm). It does not allow using the probe between tightly mounted elements. The size can be also a problem with exact positioning of the probe, especially if the field values change rapidly throughout space.

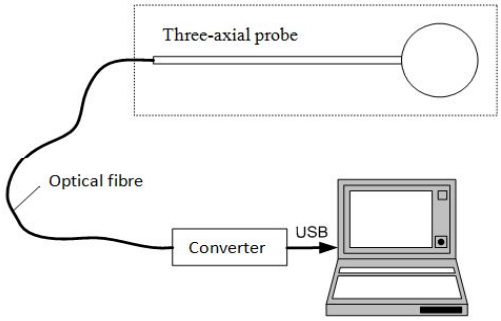

Fig. 5. Measurement system scheme

The measurement is conducted in real–time. The user interface is a dedicated software, which allows registering and imaging temporal changes in the magnitude of magnetic flux density vector or magnetic field intensity vector. Apart from data acquisition, it also offers generating reports of measurement protocol as an MS Excel file.

The meter has four measurement ranges, which can be selected via the software. The measurement range for magnetic flux density covers values from 0,2 up to 250 mT at frequencies from 50 Hz up to 10 kHz. The measurement uncertainty is below ±2% [12].

Due to non–directional measurement, the system is a convenient tool in magnetic field measurement around power transmission lines with 50 Hz currents.

Fig. 6. The magnetic field probe

4. Measurements

The measurements where performed in the lab stand at the Institute of Environmental Engineering of the Czestochowa University Technology (Fig. 7). We a used three–phase current source. The magnetic field was measured with the above mentioned measurement system. In addition, also currents were measured.

Fig. 7. Lab stand: 1 − bus bar system, 2 − three–phase current supply, 3 – PC with measurement software, 4 – magnetic field probe (inside the shield), 5 – Rogowski coils, 6 – additional measuring equipment (voltmeter, phase meter)

The position of the measurement points is shown in Fig. 8 and Fig. 9.

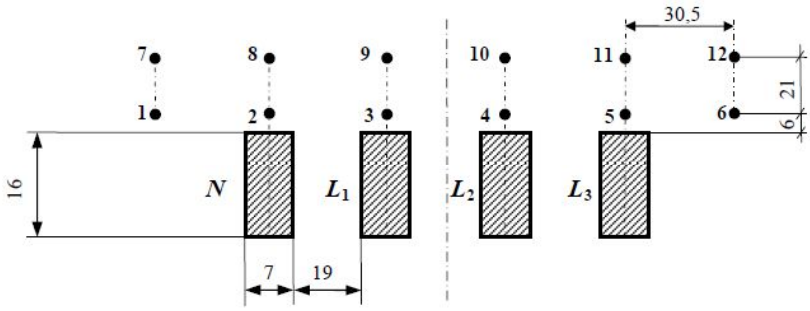

Fig. 8. The position of the measurement points of the unshielded busbar of MR type

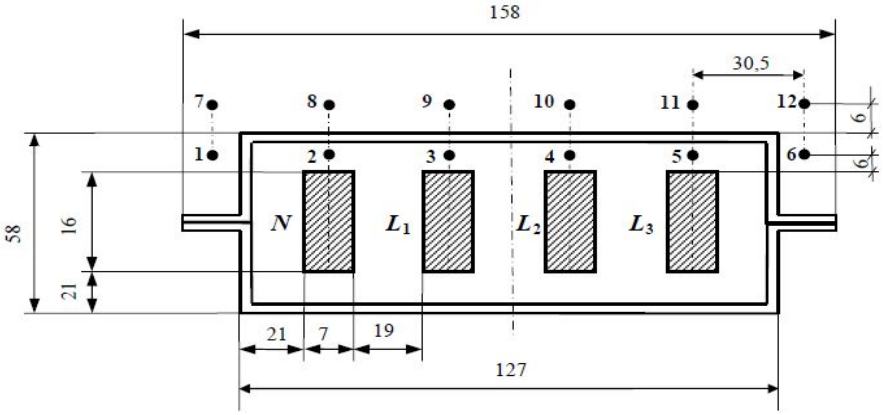

Fig. 9. The position of the measurement points of the shielded busbar of MR type

5. The scope of the investigation and the measurement results

First a symmetrical current forcing was assumed. Then, the analytical method (AM), neglecting the skin and proximity effects, the distributions of the magnetic field intensity for unshielded busbars were determined (Figs. 10, 11 and 12).

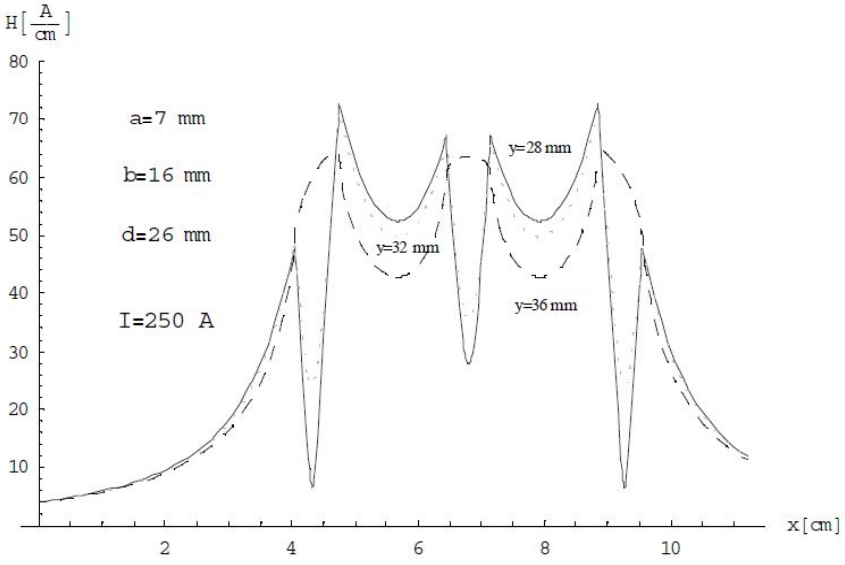

Fig. 10. The distribution of the magnetic field intensity along the *y* line = const. of the unshielded busbar of MR 250 type, with current symmetry and the *I* = 250 A current

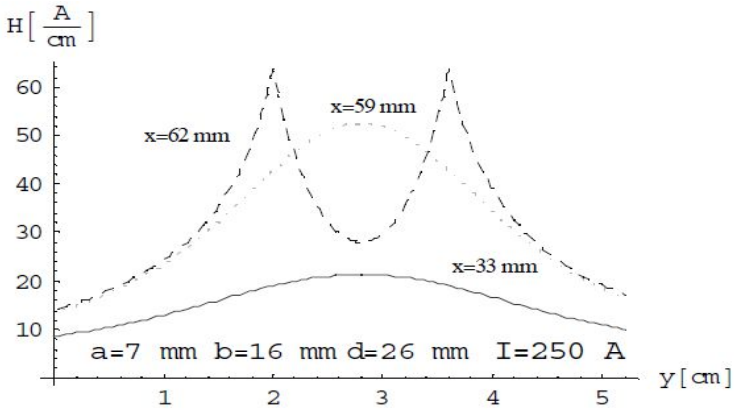

Fig. 11. The distribution of the magnetic field intensity along the x line = const. of the unshielded busbar of MR 250 type, with current symmetry and the I = 250 A current

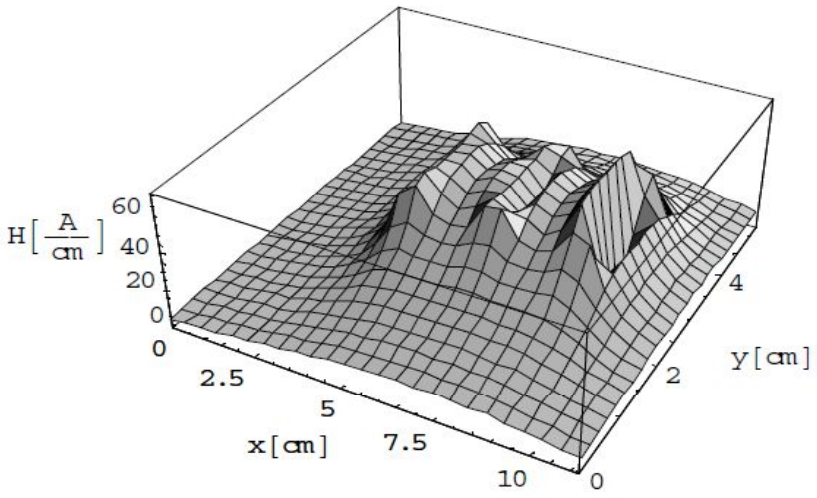

Fig. 12. The spatial distribution of the magnetic field intensity of the unshielded busbar of MR 250 type, with current symmetry and the I = 250 A current

If the skin and proximity effects are taken into account then, to determine the magnetic field intensity generated by both unshielded and shielded busbar of MR 250 type the analytical–numerical method (IEM) described in the research studies [11, 13] should be used.

For both the unshielded and the shielded busbars of MR 250 type their areas presented in the discrete form in the FEM method with the use of FEMM commercial software are shown in Fig 13 and 14.

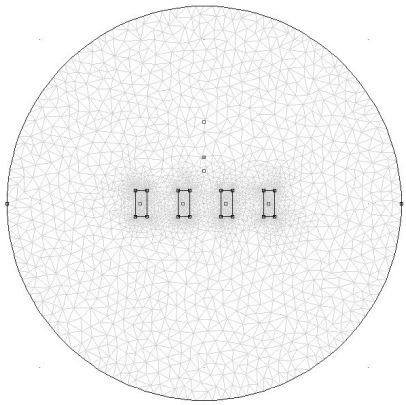

Fig. 13. The cross–section of bus bar system with FEM mesh – unshielded busbar of MR type

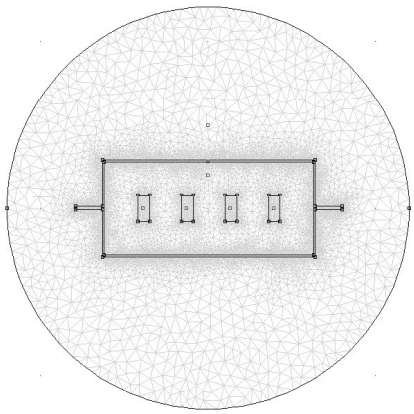

Fig. 14. The cross–section of bus bar system with FEM mesh – shielded busbar of MR type

The obtained as above distributions of the magnetic field intensity were compared with the results obtained with the use of the analytical method (AM), integral equations (IEM), finite elements (FEM) and the results of measurements (MM). That comparison was made in the selected points of both: shielded and unshielded busbar of MR type (Fig. 8 and Fig. 9) and the results are presented in Table 1.

Assuming the asymmetrical current forcing with the $\underline{I}_1 = 250\,\mathrm{e}^{-\mathrm{j}0^\circ}$, $\underline{I}_2 = 125\,I\,\mathrm{e}^{-\mathrm{j}120^\circ}$, $\underline{I}_3 = 250\,\mathrm{e}^{\mathrm{j}120^\circ}$, $\underline{I}_N = 125\,\mathrm{e}^{\mathrm{j}60^\circ}$ currents, and passing the skin and proximity effects over the distributions of the magnetic field intensity for unshielded busbar with one bar per phase and one neutral one were determined. Respective graphs are presented in Figs. 15, 16, and 17.

Table 1. The magnetic field intensity in the selected points of unshielded (*) and shielded (**) 3–phase busbar of MR type with current symmetry

Magnetic field intensity with current symmetry (in kA/m) and the I = 250 A current							
** / *	Method	Points					
		1	2	3	4	5	6
*	AM	0.314	0.972	3.077	3.068	2.782	0.450
	IEM	0.280	0.800	2.850	3.150	2.950	0.600
	FEM	0.400	1.096	4.058	4.478	4.067	0.916
	MM	0.244	0.852	3.301	3.442	3.126	0.591
**	IEM	0.250	0.650	2.850	2.450	2.850	0.550
	FEM	0.368	1.141	4.024	4.437	4.101	0.917
	MM	0.203	0.521	2.975	4.353	3.390	0.278
** / *	Method	Points					
		7	8	9	10	11	12
*	AM	0.252	0.547	0.917	0.995	0.715	0.530
	IEM	0.250	0.520	1.000	1.150	0.850	0.420
	FEM	0.339	0.697	1.244	1.483	1.248	0.619
	MM	0.225	0.565	1.035	1.218	0.957	0.443
**	IEM	0.210	0.550	1.000	1.000	0.850	0.400
	FEM	0.312	0.651	1.163	1.439	1.263	0.618
	MM	0.162	0.142	0.150	0.190	0.204	0.197

* – without enclosure; ** – with enclosure

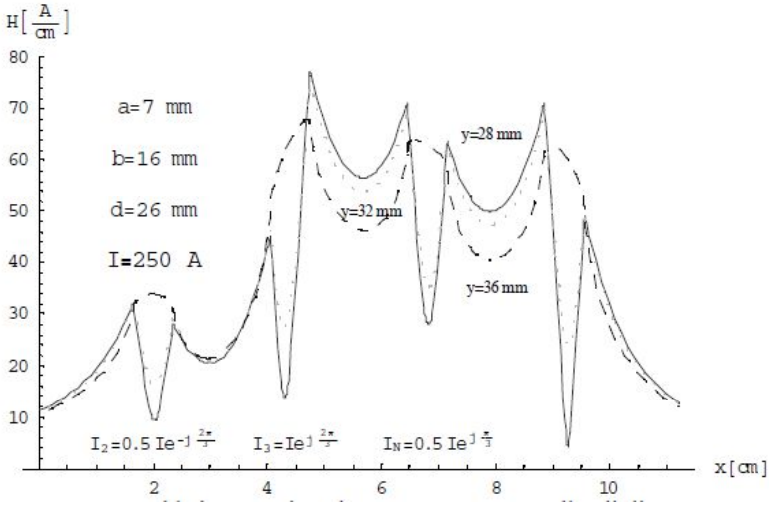

Fig. 15. The distribution of the magnetic field intensity along the y line = const. of the unshielded busbar of MR 250 type, with current asymmetry

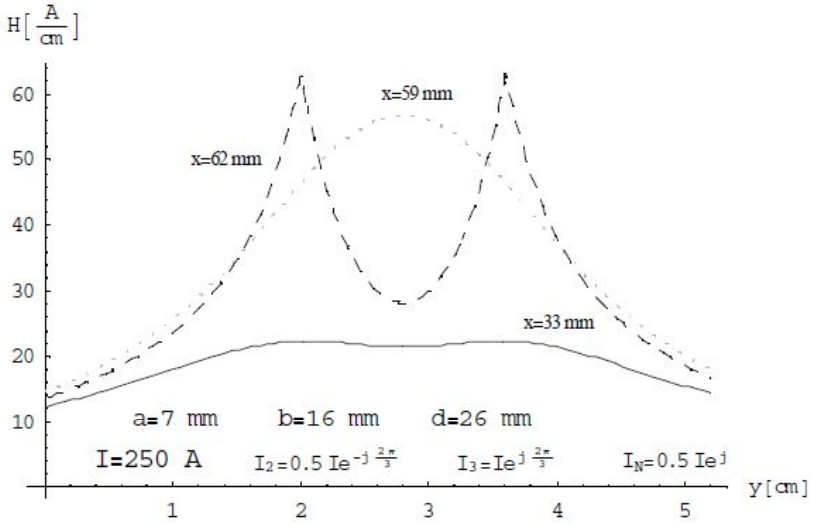

Fig. 16. The distribution of the magnetic field intensity along the *x* line = const. of the unshielded busbar of MR 250 type, with current asymmetry

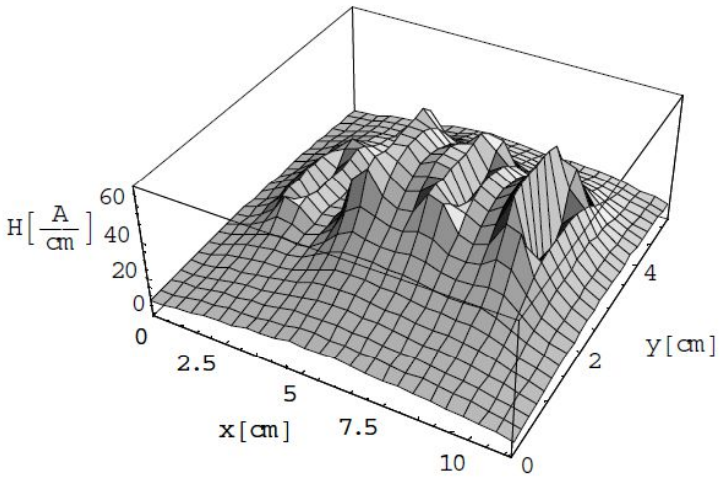

Fig. 17. The spatial distribution of the magnetic field intensity of the unshielded busbar of MR 250 type, with current asymmetry

The obtained calculated values of the magnetic field intensity with current asymmetry were compared between them and with the results obtained with the use finite elements (FEM) and the measurements (MM). That comparison was made in the selected points of both: shielded and unshielded busbar of MR type (Fig. 8 and Fig. 9) and the results are presented in Table 2.

Table 2. The magnetic field intensity in the selected points of unshielded (*) and shielded (**) 3–phase busbar of MR type with current asymmetry

Magnetic field intensity with current asymmetry (in kA/m) and the currents: $\underline{I}_1 = 250\,e^{j0^\circ}$ [A], $\underline{I}_2 = 125\,e^{-j103^\circ}$ [A], $\underline{I}_3 = 250\,e^{j135^\circ}$ [A], $\underline{I}_N = 71\,e^{j50^\circ}$ [A]							
** / *	Method	Points					
		1	2	3	4	5	6
*	AM	0.658	1.432	2.954	2.368	3.624	0.673
	IEM	0.350	1.000	2.950	2.250	3.150	0.690
	FEM	0.753	1.766	4.304	3.512	4.101	0.999
	MM	0.364	1.111	3.153	2.656	3.295	0.763
**	IEM	0.250	0.950	2.950	2.200	2.950	0.520
	FEM	0.428	1.634	3.916	3.243	4.107	0.926
	MM	0.202	1.061	3.031	3.619	3.699	0.299
** / *	Method	Points					
		7	8	9	10	11	12
*	AM	0.216	0.810	1.063	1.043	0.970	0.476
	IEM	0.280	0.500	1.000	1.050	1.000	0.450
	FEM	0.604	1.010	1.459	1.519	1.296	0.683
	MM	0.299	0.571	0.936	1.114	1.135	0.509
**	IEM	0.120	0.400	0.850	1.000	0.850	0.250
	FEM	0.346	0.728	1.128	1.329	1.220	0.616
	MM	0.151	0.137	0.142	0.184	0.217	0.236

* – without enclosure; ** – with enclosure

6. Conclusions

As the result of carried out calculations and experimental investigations a significant impact of the shield of high–current line on the distribution of the magnetic field in the proximity of busbars and in the external area of the shields was found. The specially designed and built test station enabled the experimental verification of the magnetic field in the both unshielded and shielded rectangular busbar of MR 250 type. A satisfactory conformity with the values calculated with the use of the commercial software based on the two–dimensional method of finite elements and analytical–numerical calculations was obtained. In some points the differences seem to be significant. Probably this was the effect of imprecise positioning of the probe during the measurements, and also because of the considerable size of the probe head in relation to the gap between the busbars.

References

[1] Nawrowski R.: *Tory wielkoprądowe izolowane powietrzem lub SF_6*, Wyd. Pol. Poznańskiej, Poznań 1998.

[2] Sarajcev P. and Goic R.: *Power Loss Computation in High Current Generator Bus Ducts of Rectangular Cross Section*, Electric Power Componets and Systems, No. 38, 2010, pp. 1469–1485.

[3] Szczegielniak T., Piątek Z., Kusiak D.: *Impedancje własne i wzajemne szynoprzewodów prostokątnych o skończonej długości*, Informatyka Automatyka Pomiary w Gospodarce i Ochronie Środowiska (IAPGOŚ), ISSN 2083–0157, Nr 4/2014, s. 21–24.

[4] Elektromontaż nr 2 w Katowicach: *Szynoprzewody prostokątne*. [Online]. Available: http://www.elmont2.com.pl

[5] Piątek Z., Kusiak D., Szczegielniak T.: *Pole magnetyczne szynoprzewodów prostokątnych o skończonej długości*, Wydaw. Książkowe Instytutu Elektrotechniki, Wybrane metody modelowania i symulacji, Red. K. Nita, J. Sikora, W. Wójcik i S. Wójtowicz, Warszawa – Poronin, s.28–31, 2013.

[6] Piątek Z., Baron B., Jabłoński P., Kusiak D., Szczegielniak T., *Numerical method of computing impedances in shielded and unshielded three–phase rectangular busbar systems*, Progress in Electromagnetics Research, Vol. 51, pp. 135–156, 2013.

[7] Kusiak D., Piątek Z., Szczegielniak T., Jabłoński P.: *Wyznaczanie pola magnetycznego w nieekranowanym trójfazowym czteroprzewodowym torze wielkoprądowym o szynach prostokątnych*, Electrical Engineering, Iss.81, s.55–62 , 2015.

[8] Piątek Z., Baron B., Szczegielniak T., Kusiak D., Pasierbek A.: *Numerical method of computing impedances of a three–phase busbar system of rectangular cross section*, Przegląd Elektrotechniczny, R. 89, nr 7, s. 150–154, 2013.

[9] Kusiak D., Piątek Z., Szczegielniak T., Jabłoński P.: *Obliczenia pola magnetycznego linii trójfazowej czteroprzewodowej o szynoprzewodach prostokątnych*, Electrical Engineering, Iss.85, ISSN 1897–0737, s.73–84, 2016.

[10] Piątek Z., Baron B., Jabłoński P., Szczegielniak T., Kusiak D., Pasierbek A.: *A numerical method for current density determination in three–phase bus–bars of rectangular cross section*, Przegląd Elektrotechniczny, R.89, nr 8, s. 294–298, 2013.

[11] Piątek Z., Baron B., Jabłoński P., Kusiak D., Szczegielniak T.: *Numerical method of computing impedances in shielded and unshielded three–phase rectangular busbar systems*, Progress in Electromagnetics Research (PIER), B, Vol.51, s. 135–156, 2013.

[12] Pasierbek A., Baron B., Piątek Z., Szczegielniak T., Kusiak D., *Komputerowy system pomiarowy z czujnikiem trójosiowym do pomiaru natężenia pola magnetycznego*, Prace Naukowe Politechniki Śląskiej, Elektryka, R. 58 z. 3–4 (223–224), s.61–70, 2012.

[13] Piątek Z., Baron B., Jabłoński P., Szczegielniak T., Kusiak D., Pasierbek A.: *A numerical–analytical method for magnetic field determination in three–phase busbars of rectangular cross section*, Przegląd Elektrotechniczny, R. 91, nr 12, s. 193–197, 2015.

(Received: 9. 10. 2016, revised: 16. 11. 2016)